On fatigue lifetimes and fatigue crack growth behavior of bone cement

S. ISHIHARA[1], A.J. MCEVILY[2], T. GOSHIMA[1], K. KANEKASU[3], T. NARA[1]
[1]*Department of Mechanical Engineering, Toyama University, Toyama 930, Japan*
[2]*Metallurgy Department, University of Connecticut, Storrs, CT 06269, USA*
[3]*Department of Orthopaedic Surgery, Saiseikai Takaoka Hospital, Takaoko 933, Japan*
E-mail: ishi@eng.toyama-u.ac.jp

Bone cement is used to develop a mechanical bond between an artificial joint and the adjacent bone tissue, and any degradation of this bond is of serious concern since it can lead to loosening and eventually malfunction of the artificial joint. In the present study, the fatigue lives and fatigue crack propagation behavior of two bone cements, CMW Type 3 and Zimmer, were investigated, and it was found that the size and distribution of pores played a major role in influencing both the fatigue crack initiation and propagation processes. The fatigue lifetimes of CMW exceeded those of Zimmer because of a lesser density of large pores. When the fatigue lifetimes were plotted as a function of K_{limax}, the maximum initial stress intensity factor based upon the initiating pore size, the difference in fatigue lifetimes between CMW and Zimmer bone cements was greatly reduced. The fatigue crack growth behavior of both bone cements were similar. This is a further indication that the noted differences in fatigue lifetimes were related to the size of the pore at the crack initiating site.

1. Introduction

Bone cement is used to develop a mechanical bond between an artificial joint and the adjacent bone tissue, and any degradation of this bond is of serious concern since it can lead to loosening and eventually malfunction of the artificial joint. One of the ways by which this degradation can occur is through fatigue failure of the bone cement itself. The average person takes about 1 000 000 steps in one year, and hence in a hip joint, of the order of 10^6 fatigue cycles per year are applied to the bone cement. Although it is therefore important that the fatigue characteristics of bone cement be understood, only a few studies of the fatigue properties of bone cement have been performed thus far.

In one such study, Freitag and Cannon [1] carried out rotating bending fatigue tests of a bone cement in air at 295 K and also in a physiological salt solution at 310 K. The cyclic stress amplitudes were low, ranging from 14 to 41 MPa at a frequency of 20 Hz. They found the fatigue lives in air to be shorter compared to those in salt solution. In another study, Cipolletti and Cooke [2] carried out zero-tension fatigue tests of bone cement in a physiological salt solution at 310 K at a cyclic frequency of 1 Hz. At a stress amplitude of 13 MPa the fatigue life was about 10^4 cycles, and at 6 MPa the fatigue life was about 10^6 cycles. Carter *et al*. [3] carried out static tensile tests and tension-compression fatigue experiments of bone cement in a physiological salt solution at 310 K at a strain rate of 0.02/s. They found that because of the viscoelastic nature of bone cement, the fatigue lives were strongly dependent on strain amplitude rather than stress amplitude. They also observed that porosity within the bone cement, as determined from X-ray photographs, strongly affected both the tensile strength and the fatigue strength of the specimens. This porosity has been shown by Bayne *et al*. [4] to be due to air inclusions which are inevitably introduced during the mixing procedure. Burke *et al*. [5] used centrifugation and Linden and Gillquist [6] used vacuum mixing as techniques to create a cement of less porosity and better mechanical properties. Davies *et al*. [7] determined both the static tensile and fatigue properties of three types of bone cement; Simplex P, LVC, and Zimmer Regular bone cement. Although there was no significant difference in tensile strengths, the fatigue properties of Simplex P were found to be superior to the fatigue properties of LVC and Zimmer Regular bone cements.

The present research further investigates the fatigue properties of bone cement, with both fatigue lifetimes and fatigue crack growth behavior being studied. The fatigue tests were carried out in four-point-bending in Ringer's solution (0.86 w/o NaCl, 0.033 w/o $CaCl_2$, 0.03 w/o KCl, balance H_2O) and in air at two frequencies, 1 Hz and 20 Hz. Two different types of commercial bone cements were used, CMW Type 3 and Zimmer low viscosity cement. Since porosity was present in both bone cements, the influence of porosity on the fatigue characteristics of bone cements was also studied.

TABLE I Chemical compositions of the materials used

	CMW	Zimmer
Powder	Methyl methacrylate Barium sulfate Benzoyl peroxide	Methyl methacrylate Barium sulfate Benzoyl peroxide
Liquid	Methyl methacrylate N, N-Dimethyl-p-toluidene Hydroquinone Ascorbic acid Ethyl alcohol	Methyl methacrylate N, N-Dimethyl-p-toluidene Hydroquinone

2. Specimens and experimental procedures

2.1. Specimens

The bone cements used in the present experiments were CMW Type 3 produced by CMW Laboratories, and Zimmer low-viscosity cement produced by the Bristol-Myers Squibb Company. In the following we will refer to these two bone cements as CMW and Zimmer. Table I gives the chemical compositions. As seen from Table I, the chemical formulations of the two bone cements are quite similar, but the relative amounts of each constituent are proprietary information.

The specimens were manufactured by first mixing twenty weight parts of powder with nine weight parts of liquid in accord with instructions contained in each company's operation manual. After manually stirring the powder and liquid mixture for 1.5 min, the mixture was poured into a steel mold of proper size to shape the specimens. When each specimen had completely solidified, it was taken out of the mold and then ground to the final specimen size shown in Fig. 1. To facilitate the observation of fatigue cracks, the upper surface of each specimen was then polished to a mirror finish by using both emery paper (#1000 $\sim$ 1500) and diamond paste.

2.2. Experimental methods

The mechanical properties, i.e. Young's modulus, bending strength, and fracture toughness, were determined in four-point-bending with an inner span length of 10 mm and an outer span length of 30 mm. The results obtained in three tests of each specimens as well as the average values are given in Table II. It is noted that the modulus of CMW was lower than that of Zimmer, but the bending strength was higher. The fracture toughness values were similar.

The four-point-bending fatigue tests were carried out under $R = 0.1$ loading conditions in an electro-hydraulic, closed-loop fatigue testing machine at frequencies of 1 and 20 Hz, utilizing a sine waveform. In order that the experiments were carried out in the same environment as in a living body, the fatigue experiments were performed in Ringer's solution maintained at a constant temperature of 310 K. The Ringer's solution was prepared one hour before testing. Additional experiments were performed in laboratory air for a comparison with those in Ringer's solution. The time between specimen preparation and testing was less than two days. Successive observations of the specimen surface during the fatigue process were performed by interrupting the test periodically, and any cracks that appeared on the specimen surface were measured in situ with an optical microscope at 400 times magnification. Since porosity in bone cement is known to affect fatigue behavior, the distributions of the diameters of pores on polished surfaces as well as the distributions of their two-dimensional projected areas were determined with the aid with an optical microscope.

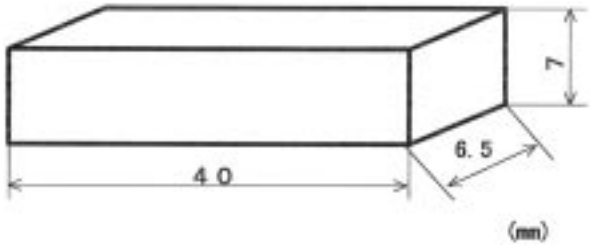

Figure 1 Shape and dimensions of the specimen used.

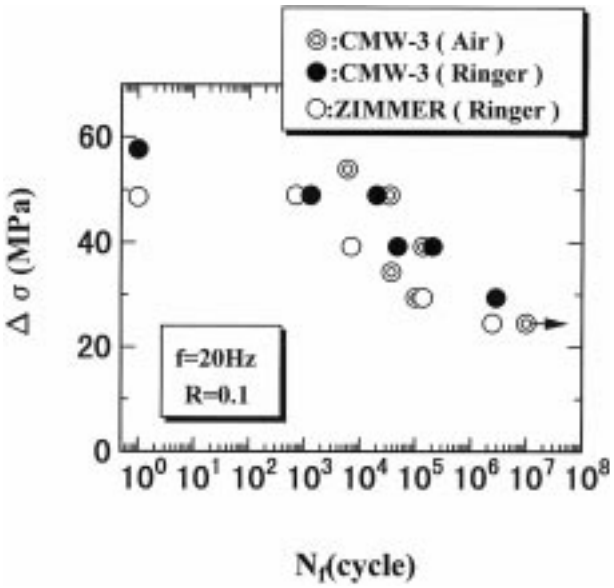

Figure 2 S–N results of CMW and Zimmer bone cements obtained at 20 Hz in Ringer's solution at 310 K. Also shown are results for CMW tested in air at 295 K.

3. Experimental results

3.1. S–N curves of CMW and Zimmer bone cements

Fig. 2 shows the relationship between stress range, $\Delta\sigma$, and number of cycles to failure, N_f, for CMW and Zimmer bone cements tested at a frequency of 20 Hz in Ringer's solution. Also shown for comparison are the

TABLE II Mechanical properties of the materials used

	CMW			(mean)	ZIMMER			(mean)
Young's modulus (GPa)	2.62	2.75	2.68	2.69	2.94	2.85	2.94	2.92
Bending strength (MPa)	59.24	55.84	57.93	57.67	48.43	49.97	47.51	48.65
Fracture toughness (MPam$^{1/2}$)	2.17	2.21	2.28	2.22	2.19	2.09	2.15	2.14

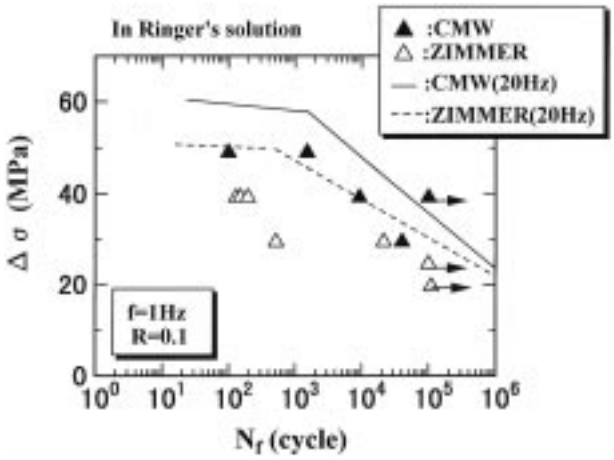

Figure 3 S–N results for CMW and Zimmer bone cements obtained at 1 Hz in Ringer's solution at 310 K. Results obtained at 20 Hz are shown for comparison.

results for CMW bone cement tested in laboratory air, and it is seen that no obvious difference in fatigue lives exists between the test results obtained in laboratory air and those obtained in Ringer's solution. Upon comparing the results for CMW and Zimmer, it is seen that the fatigue lives of CMW bone cement are greater than those for Zimmer, especially in the high stress, low cycle region, a reflection of the higher strength of the CMW.

Fig. 3 shows the fatigue results for CMW and Zimmer which were obtained at 1 Hz in Ringer's solution at 310 K. In this figure, the S–N curves for CMW and Zimmer obtained at $f = 20$ Hz are also shown as solid and broken lines, respectively. It is seen that at 1 Hz the fatigue lives of CMW are longer than those of Zimmer, as at 20 Hz. More significantly, the fatigue lives for both bone cements at 1 Hz are shorter by 1 to 2 orders of magnitude as compared with fatigue lives at 20 Hz, a clear indication that an influence of frequency on fatigue lives exists.

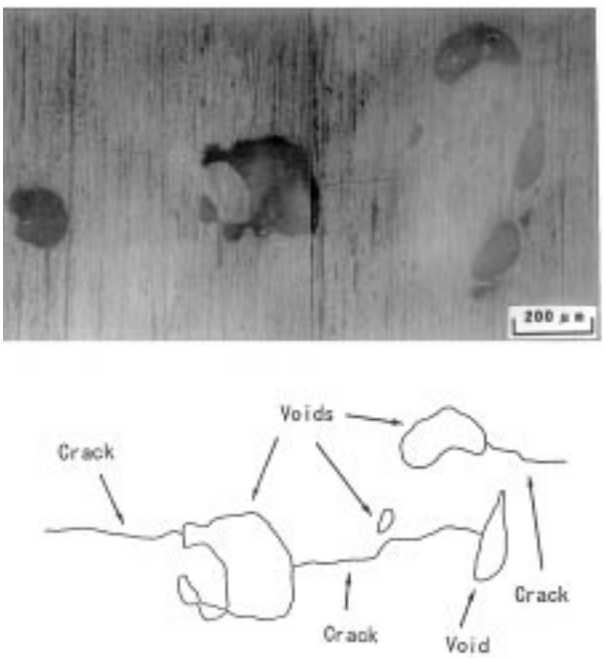

Figure 4 Crack propagation process as observed during fatigue process in CMW.

3.2. Fatigue crack initiation and growth behavior of bone cement

Fig. 4 shows a typical crack growth process as observed in this case for CMW during fatigue testing of bone cement. A schematic illustration is also attached to the figure to clarify the process. As seen from Fig. 4, cracks initiate and propagate from a number of pores located at the specimen surface. Several of these cracks are arrested when they encounter other pores during propagation. These arrested cracks propagate again if reinitiation occurs at the arresting pore, or if another crack coalesces with the arrested crack. Final failure of the specimen occurs by the coalescence of several cracks.

From such observations of the specimen surfaces as well as the fracture surfaces, it became clear that all fatigue cracks initiated at pores that were present on the specimen surface or immediately below the specimen surface. If we consider the initiating pore to be equivalent to a crack, we can evaluate an equivalent initial maximum stress intensity factor, K_{Iimax}, for the pore using the following expression proposed by Murakami *et al.* [8].

$$K_{Iimax} = 0.65\,\sigma_{max}\{\pi\sqrt{area}\}^{1/2} \quad (1)$$

$$K_{Iimax} = 0.50\,\sigma_{max}\{\pi\sqrt{area}\}^{1/2} \quad (2)$$

where the area is the pore area at which fatigue cracking occurs. The initial stress intensity factor was calculated using Equation 1 when the hole was on the specimen surface, or using Equation 2 when it was inside the specimen. The S–N data were then converted to a relation between the initial stress intensity factor K_{Iimax} and the fatigue life, N_f.

Fig. 5 shows the relationship between K_{Iimax} and N_f for both CMW and Zimmer at 20 Hz in Ringer's solution at 310 K. Fig. 6 is similar to Fig. 5, but with $f = 1$ Hz. A better correlation is observed between K_{Iimax} and N_f than between $\Delta\sigma$ and N_f shown in Figs 2 and 3. The scatter of the data is also observed to be less pronounced in Figs 5 and 6 as compared to Figs 2 and 3. Also, the difference between CMW and Zimmer seen in Figs 2 and 3 is largely eliminated in Figs 5 and 6. This finding indicates that the differences observed between CMW and Zimmer

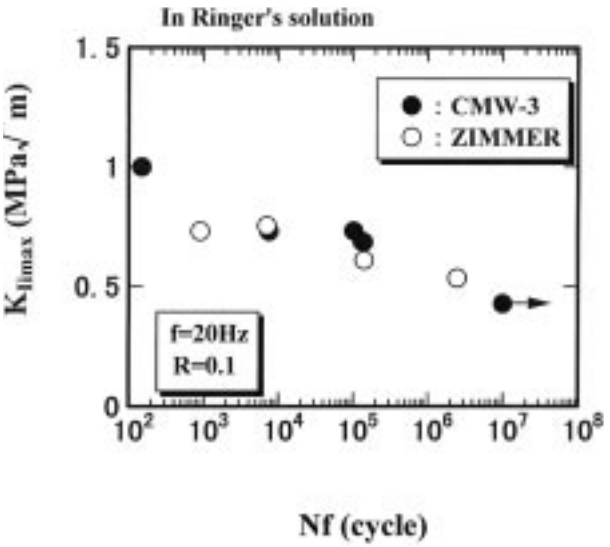

Figure 5 Relationship between K_{Iimax} and N_f at 20 Hz.

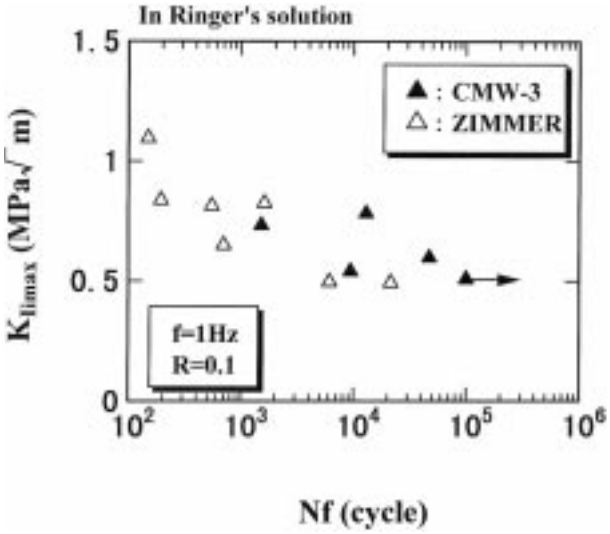

Figure 6 Relationship between K_{limax} and N_f at 1 Hz.

in Figs 2 and 3 are largely due to differences in the distribution of pore sizes.

3.3. Fatigue crack growth behavior of bone cements

Fig. 7 shows the relation between the crack growth rate dc/dN, where c is the half-length of a surface crack, and the stress intensity factor range ΔK for the CMW and Zimmer bone cements. These data were obtained at 20 Hz in Ringer's solution maintained at 310 K. Fig. 8 shows similar results at 1 Hz. In these figures, the values of ΔK were calculated using the following expression, on the assumption that the crack shape is semicircular during the growth process.

$$\Delta K = 0.65\,\Delta\sigma\sqrt{\pi c} \tag{3}$$

As seen from Figs 7 and 8, an almost linear relationship between dc/dN and ΔK exists on the log–log plot, such

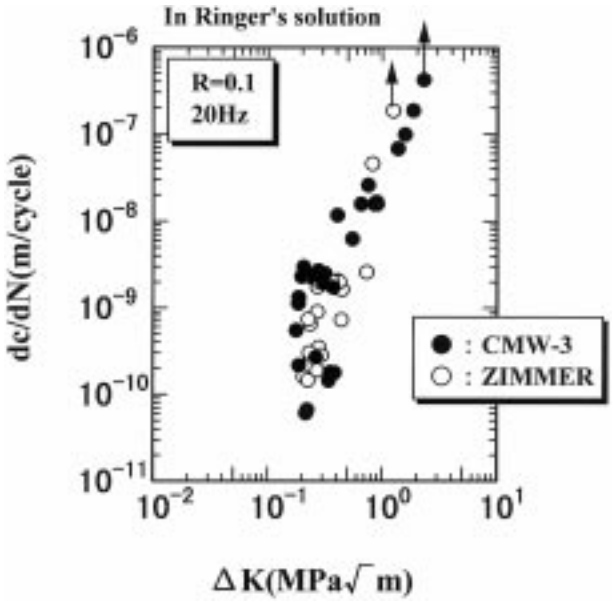

Figure 7 Relationship between dc/dN and ΔK at 20 Hz.

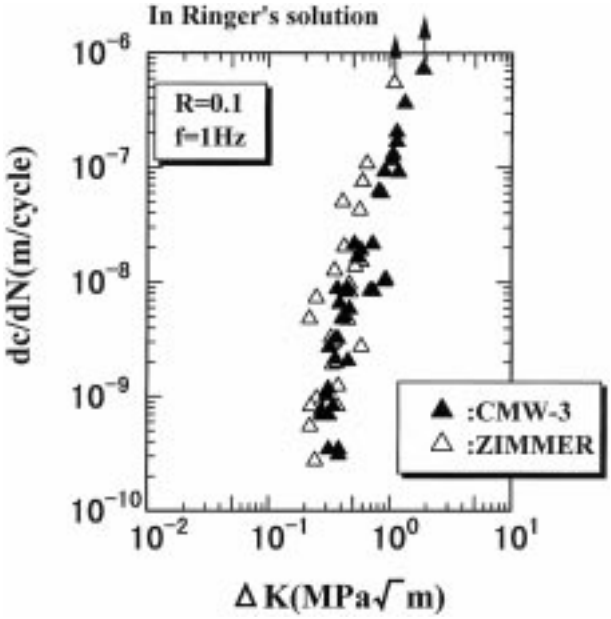

Figure 8 Relationship between dc/dN and ΔK at 1 Hz.

that the following Paris's law holds, as in the case of metallic materials above the near-threshold region.

$$\mathrm{dc/dN} = C(\Delta K)^{\mathrm{m}}, \tag{4}$$
$$\text{where } C = 7.6 \times 10^{-8} \text{ and } m = 3.6$$

No significant difference between the fatigue crack growth behavior of CMW and Zimmer was observed. Upon comparing Figs 7 and 8 it is seen that below a crack growth rate of 10^{-8} m/cycle there is little effect of frequency on the rate of fatigue crack growth. However, above this rate, crack propagation at 1 Hz is higher than at 20 Hz. These results also suggest that the differences noted with respect to material and frequency particularly in the high cycle fatigue range of Figs 2 and 3 may be associated with differences in pore size distributions as well as to the viscoelastic nature of bone cements.

3.4. Area and diameter distributions of pores at specimen surface

When specimens are produced by mixing the powder and liquid components, pores of various sizes are formed within the specimens during the solidification process. Since these pores are known to affect the fatigue process [3], the size and density of the pores present in the specimens used in this investigation were determined by examining the pore distributions on the cross-sections of three specimens. Total observed area was $137 \sim 150\,\mathrm{mm}^2$.

Fig. 9 indicates the probabilistic distributions of areas and diameters of the holes that are included in cross-sections of the specimens made of CMW and Zimmer. The data are plotted on Weibull probability paper by the average rank method. The total number of pores observed was about 200. As seen from Fig. 9, the pore diameters ranged from 10 μm to 1000 μm, so that there is a large variation in pore size, with some rather large pores being present. However, a clear difference between

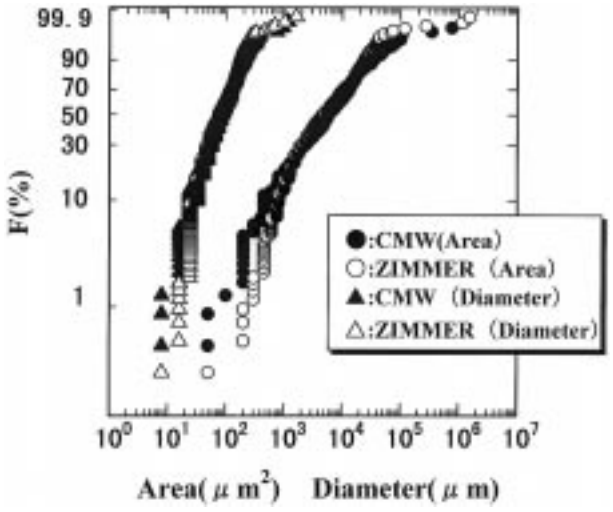

Figure 9 Weibull plots of the distributions of areas and diameters of holes in the specimens made of CMW and Zimmer.

CMW and Zimmer cannot be seen in the distributions of hole sizes.

Since the largest pores are of greatest concern, the distribution of pores whose diameter exceeds 300 μm is shown in Fig. 10. As seen from this figure, the probability that 300 μm or large pores are present within a specimen is higher for Zimmer than CMW, which is somewhat unexpected since the Zimmer has a lower viscosity than CMW. However, the total number of pores observed per unit area for CMW was 1.56/mm^2, and for Zimmer was 0.96/mm^2.

4. Discussion

4.1. On the difference in fatigue lives between CMW and Zimmer

The experimental results indicate that in the present experiments the fatigue life of CMW is greater than that of Zimmer. The principal factor that is responsible for this difference appears to be the higher bending strength of the CMW specimens. This difference may result from a lesser amount of pores greater than 300 μm in diameter in the CMW than in the Zimmer, as shown in Fig. 10. Fatigue cracks initiated at the larger pores will propagate more rapidly and hence reduce the fatigue life as compared to those cracks initiated at smaller pores simply because of their greater effective crack size. It is also noted that the observed differences in pore sizes and strength values are a function of the mixing technique. For example, Linden and Gillquist [6] found the compressive and shear properties of Zimmer cement to be improved by mechanical rather than by manual mixing, probably because of a decrease in porosity size.

4.2. Effect of stress frequency on fatigue behavior of bone cement

The fatigue lives of bone cement at 1 Hz are less than those at 20 Hz, although the fatigue crack growth rates, except at the higher growth rates, were similar. This suggests that the effect of frequency on fatigue life has more to do with the crack initiation process than the crack propagation process. It is known that bone cements are viscoelastic materials, so that more strain develops at low frequency as compared to high. A higher local strain at the initiating pore due to a lower frequency will promote crack initiation, and hence have an adverse effect on fatigue life.

4.3. Comparison of fatigue process of metallic materials with that of bone cements

It is of interest to compare the fatigue lives of bone cement with those of a metallic material. For this purpose the stress range for CMW and Zimmer bone cements is expressed in non-dimensional form as $\Delta\sigma/\sigma_B$ where σ_B denotes a bending strength of the material, and the fatigue lifetimes are plotted in terms of this parameter in

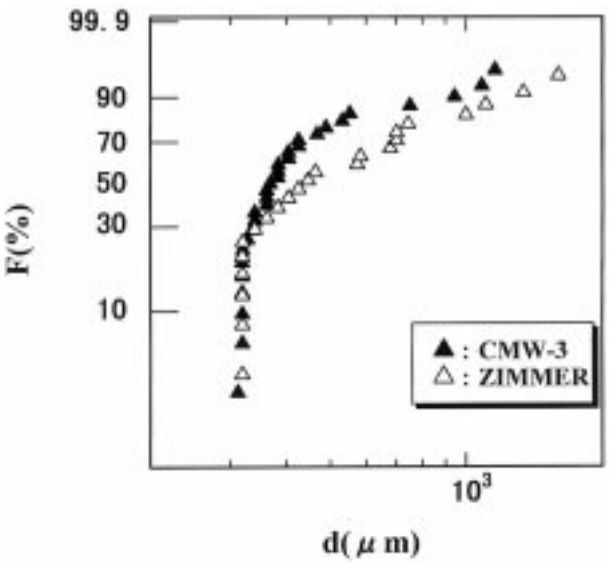

Figure 10 Diameter distributions of pores (> 300 μm) for both CMW and Zimmer plotted on Weibull probability paper.

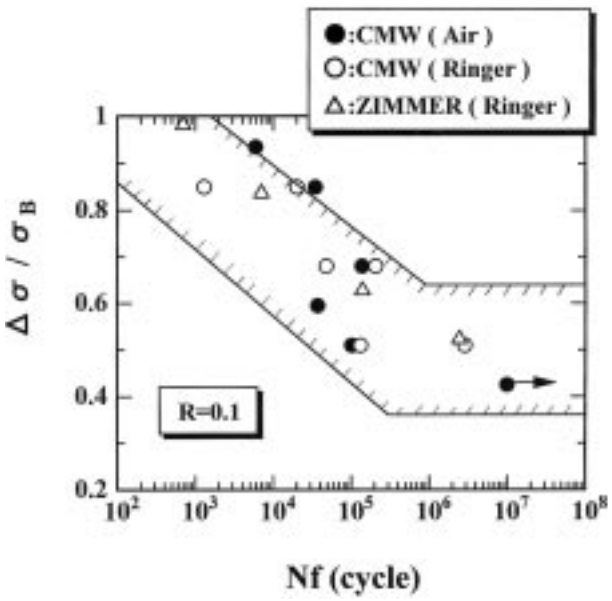

Figure 11 Relationship between $\Delta\sigma/\sigma_B$ where σ_B denote a bending strength of the material, and the fatigue lifetimes Nf for both CMW and Zimmer bone cements.

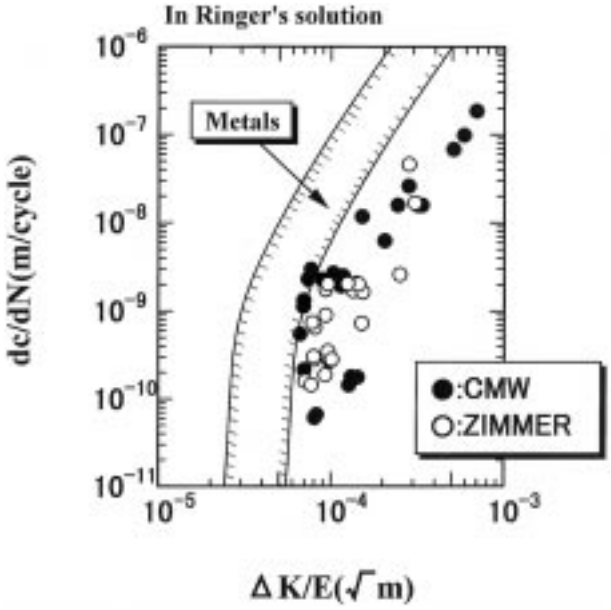

Figure 12 Relationship between dc/dN and Δ K/*E*, where *E* is Young's modulus of the material.

Fig. 11. For comparison, the cross-hatched area in the figure indicates the range of $\Delta\sigma/\sigma_B$ and N_f for structural steel [9]. In Fig. 11 there is not a clear difference between structural steel and bone cement, perhaps because the cross-hatched area covers such a wide range.

A more meaningful comparison can be made with respect to fatigue crack propagation. For this purpose Fig. 5 was replotted in terms of Δ K/E, where E is Young's modulus, as shown in Fig. 12. In Fig. 12, the usual range for metallic materials [10] is indicated by the cross-hatched area. As seen from this figure, the crack growth rate of a bone cement at a constant value of Δ K/E compares favorably with that of metallic materials. This situation may develop as the result of the crack-arresting effect of the pores contained within bone cements which serve to retard the crack growth process.

5. Conclusions

In the present study, the fatigue lives and fatigue crack propagation behavior of two bone cements, CMW type 3 and Zimmer, were investigated, and it was found that the size and distribution of pores played a major role in influencing both the fatigue crack initiation and propagation processes.

In addition, the following conclusions were reached:

1. The fatigue lifetimes of CMW exceeded those of Zimmer because of a lesser density of large pores.
2. When the fatigue lifetimes were plotted as a function of K_{limax}, the maximum initial stress intensity factor based upon the initiating pore size, the difference in fatigue lifetimes between CMW and Zimmer bone cements was greatly reduced, as was the degree of scatter in test results.
3. There was little effect of the environment, i.e. air vs. Ringer's solution, on the fatigue lifetimes.
4. The fatigue crack growth behavior of both bone cements were similar. This is a further indication that the noted differences in fatigue lifetimes were related to the size of the pore at the crack initiating site.
5. A decrease in test frequency from 20 Hz to 1 Hz resulted in a decrease in fatigue lifetime, and to a lesser degree to an increase in the rate of fatigue crack growth.
6. The growth rate of surface fatigue cracks in bone cement was less than the fatigue crack growth rate in steel when compared on the basis of ΔK/E. This circumstance was attributed to the beneficial arresting effect of pores in bone cement.

References

1. T. A. FREITAG and S. CANNON, *J. Biomed. Mater. Res.* **11** (1977) 609.
2. G. B. CIPOLLETTI and F. W. COOKE, Trans. of the 4th Annual Meeting of the Society for Biomaterials, **2** (1978) 134.
3. D. R. CARTER, E. I. GATES and W. H. HARRIS, *J. Biomed. Mater. Res.* **16** (1982) 647.
4. S. C. BAYNE, E. P. LAUTENSCHLAGER, C. L. COMPERE and R. WILDES, *ibid.* **9** (1975) 27.
5. D. W. BURKE, E. I. GATES and W. H. HARRIS, *J. Bone Joint Surg.* **66-A** (1984) 1265.
6. U. LINDEN and J. GILLQUIST, *Clin. Orthop.* **247** (1989) 148.
7. J. P. DAVIES, D. O. O'CONNOR, J. A. GREER and W. H. HARRIS, *J. Biomed. Mater. Res.* **21** (1987) 719.
8. Y. MURAKAMI, S. KODAMA and S. KONUMA, *Trans. Japan Soc. Mech. Engrs.* **54-A** (1988) 688.
9. Data Book on Metal Fatigue, *Japan Soc. Mech. Engnrs*, (1961) p. 64.
10. S. USAMI, in ''Fatigue thresholds'', edited by J. Backlund, A. F. Blom and C. J. Beevers, (EMAS Publishers, UK, 1981) p. 290.

Received 28 July
and accepted 12 November 1998